8564 *Biochemistry* **2010,** *49,* 8564–8576
DOI: 10.1021/bi1012029

BIOCHEMISTRY
including biophysical chemistry & molecular biology
Article

Enzymatic Processing of Fumiquinazoline F: A Tandem Oxidative-Acylation Strategy for the Generation of Multicyclic Scaffolds in Fungal Indole Alkaloid Biosynthesis[†]

Brian D. Ames, Xinyu Liu,[‡] and Christopher T. Walsh*

Department of Biological Chemistry and Molecular Pharmacology, Harvard Medical School, 240 Longwood Avenue, Boston, Massachusetts 02115. [‡]*Current address: Department of Chemistry, University of Pittsburgh, 219 Parkman Ave., Pittsburgh, PA 15232.*

Received July 29, 2010; Revised Manuscript Received August 26, 2010

ABSTRACT: *Aspergillus fumigatus* Af293 is a known producer of quinazoline natural products, including the antitumor fumiquinazolines, of which the simplest member is fumiquinazoline F (FQF) with a 6-6-6 tricyclic core derived from anthranilic acid, tryptophan, and alanine. FQF is the proposed biological precursor to fumiquinazoline A (FQA) in which the pendant indole side chain has been modified via oxidative coupling of an additional molecule of alanine, yielding a fused 6-5-5 imidazoindolone. We recently identified fungal anthranilate-activating nonribosomal peptide synthetase (NRPS) domains through bioinformatics approaches. One domain previously identified is part of the trimodular NRPS Af12080, which we predict is responsible for FQF formation. We now show that two adjacent *A. fumigatus* ORFs, a monomodular NRPS Af12050 and a flavoprotein Af12060, are necessary and sufficient to convert FQF to FQA. Af12060 oxidizes the 2′,3′-double bond of the indole side chain of FQF, and the three-domain NRPS Af12050 activates L-Ala as the adenylate, installs it as the pantetheinyl thioester on its carrier protein domain, and acylates the oxidized indole for subsequent intramolecular cyclization to create the 6-5-5 imidazolindolone of FQA. This work provides experimental validation of the fumiquinazoline biosynthetic cluster of *A. fumigatus* Af293 and describes an oxidative annulation biosynthetic strategy likely shared among several classes of polycyclic fungal alkaloids.

Filamentous fungi are prolific producers of bioactive secondary metabolites, including potent mycotoxins such as aflatoxin, ochratoxin, gliotoxin, and cyclopiazonic acid (*1*), and molecules of important therapeutic value such as the antibiotic cephalosporins/penicillins, immunosuppressant cyclosporins, and cholesterol-lowering statins. One class of fungal natural products consists of the quinazoline alkaloids (*2*, *3*), a subclass of which are the fumiquinazolines (FQs) which possess a pyrazino[2,1-*b*]quinazoline-3,6-dione core scaffold derived from condensation of anthranilic acid (Ant) with two additional amino acids (Figure S1 of the Supporting Information) (*4*).

The isolation and structures of seven fumiquinazolines (A−G), produced by a strain of *Aspergillus fumigatus* separated from the gastrointestinal (GI) tract of the saltwater fish *Pseudolabrus japonicas*, were originally described in an effort to discover cytotoxic compounds from marine microorganisms (*5*). More recently, analysis of secondary metabolites produced by 40 strains of *A. fumigatus*, including strain Af293 relevant to this work, demonstrated that the fumiquinazolines make up one of three families of secondary metabolites isolated from all tested strains (*6*). In addition to their widespread production in *A. fumigatus*, the isolation of FQs has also been reported in several *Penicillium* species (*7*). The FQs are moderately cytotoxic and have been reported to exhibit antitumor activity against several cancer cell lines (*8*). Related pyrazinoquinazolinone metabolites have been isolated from various fungi: fumiquinazoline H-I (*Acremonium* sp.) (*9*), fiscalins A and B (*Neosartorya fischeri*) (*10*), glyantrypine (*Aspergillus clavatus*) (*11*), cottoquinazoline A (*Aspergillus versicolor*) (*12*), alantrypinone (*Penicillium thymicola*) (*13*), spiroquinazoline (*Aspergillus flavipes*) (*14*), and verrucines (*Penicillium verrucosum*) (*15*, *16*) (Figure S1 of the Supporting Information). Despite the widespread production of pyrazinoquinazolinones by filamentous fungi and their isolation based on bioactivity-guided approaches, their role in the chemical ecology of the producing organism is yet to be determined.

The construction of the core scaffold of di- and tripeptidyl alkaloids may be accomplished by nonribosomal peptide synthetase (NRPS) assembly lines (*17*−*19*). NRPSs are often found as multidomain megasynthases composed minimally of adenylation (A), carrier protein/thiolation (T), and condensation (C) domains arranged in repeating units termed modules. The general process of building peptidyl frameworks begins with A domain-catalyzed activation of amino acid building blocks as acyl-AMPs. The acyl group of the acyl adenylate is then attached to the 4′-phosphopantetheine (ppt) prosthetic group of the T domain to form an acyl−thioester intermediate. T domain-tethered intermediates are then delivered to the active site of a C domain, which catalyzes the coupling of building block units via amide bond formation. Modifying domains sometimes present as part of the NRPS include the C domain variant epimerization (E) and heterocyclization domains and domains for N-methylation or formylation. Following maturation and in-line modification of the growing peptide chain, several mechanisms exist for chain

[†]This work was supported in part by National Institutes of Health Grant GM20011 (to C.T.W.), F32GM090475 (postdoctoral fellowship to B.D.A.), and the Ernst Schering Foundation (postdoctoral fellowship to X.L.).

*To whom correspondence should be addressed: Department of Biological Chemistry and Molecular Pharmacology, Harvard Medical School, 240 Longwood Ave., Boston, MA 02115. E-mail: christopher_walsh@hms.harvard.edu. Phone: (617) 432-1715. Fax: (617) 432-0438.

 Published on Web 08/30/2010

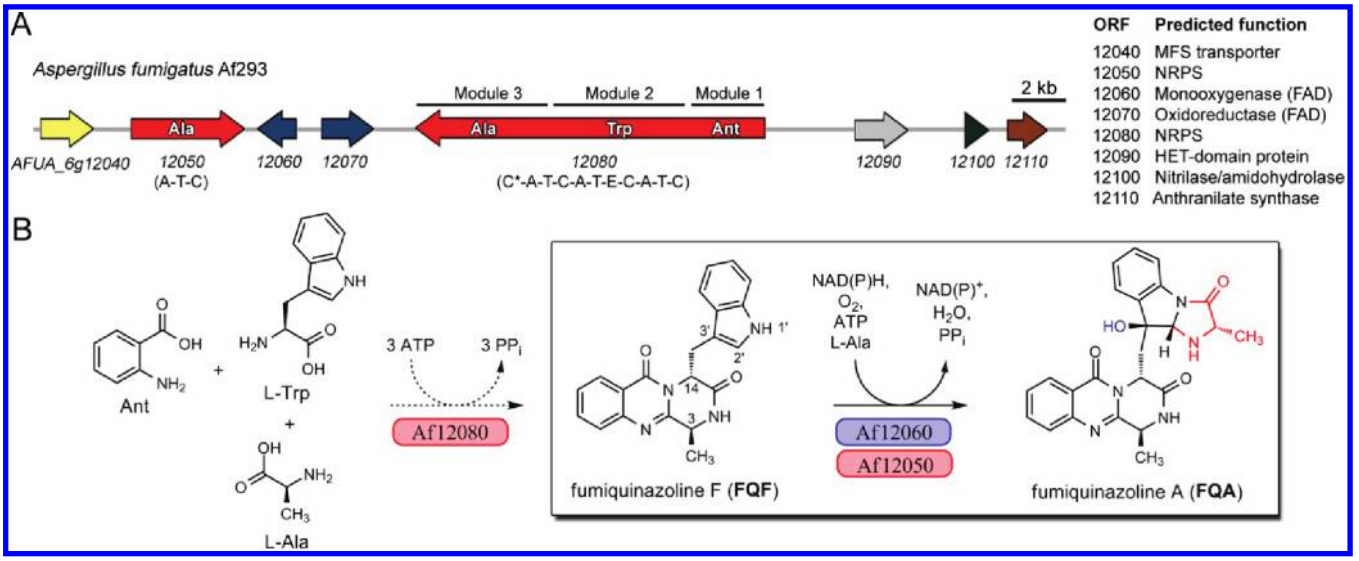

FIGURE 1: (A) Fumiquinazoline gene cluster and (B) proposed biosynthetic route to fumiquinazoline A in *A. fumigatus* Af293.

release (*20*, *21*). In bacterial NRPSs, and in the fungal ACV tripeptide synthetase, a terminal thioesterase (TE) domain catalyzes chain release via hydrolysis or macrocyclization. A distinguishing feature of many fungal NRPSs is the absence of a terminal TE domain and instead the presence of a terminal condensation, reductive, or thiolation domain (*19*). Particularly relevant to the construction of the FQs and related fungal alkaloids is the fact that the terminal C domains may use intra- or intermolecular nucleophiles to attack the thioester bond of an enzyme-tethered intermediate for chain release via cyclization. Additionally, during chain elongation and after chain release, the peptidyl scaffold is often modified by the action of discrete tailoring enzymes (*22*, *23*).

Because of the medicinal relevance of *A. fumigatus* as an allergen and opportunistic pathogen in humans (*24*), this organism was among the first of its genus to be sequenced. To date, two clinical isolates of *A. fumigatus* have been sequenced: strain Af293 (FGSC A110) (*25*) and strain CEA10 (FGSC A1163) (*26*). The availability of sequenced fungal genomes has greatly facilitated the identification of secondary metabolite gene clusters through genome mining (*27*). On the basis of this approach, we recently identified putative anthranilate-activating NRPS modules in the genomes of *Aspergilli* (*28*).

Biochemical characterization of module 1 of AFUA_6g12080 from *A. fumigatus* Af293 (abbreviated as Af12080) validated its anthranilate-dependent adenylation and thiolation activities and prompted us to propose it as part of an eight-gene cluster involved in fumiquinazoline biosynthesis (Figure 1A) (*28*). Modules 2 and 3 of Af12080 are predicted to activate and load Trp and Ala, respectively, providing for the assembly of an Ant-Trp-Ala-S-enzyme intermediate that would undergo double cyclization for chain release and generation of the tricyclic 6-6-6 product fumiquinazoline F (Figure 1B) (*28*). The presence of an E domain predicted for module 2 of Af12080 is consistent with epimerization of L-Trp to D-Trp during assembly to generate the *R*-stereocenter at C14 of FQF. Maturation of FQF to FQA would involve further processing of the Trp side chain indole group through oxidative coupling of L-Ala to give a 6-5-5 framework known as an imidazoindolone (Figure 1B).

One strategy for accomplishing the net oxidation, acylation, and cyclization for FQA assembly would be to utilize an NRPS module to activate and install L-Ala as an S-pantetheinyl thioester on the holo form of a T domain and catalyze amide bond formation by directed attack of the indole NH group of FQF on the activated alanyl thioester carbonyl. Oxidation of the indole C2′−C3′ bond could prime it for N-acylation and intramolecular cyclization en route to formation of FQA. Consonant with this proposal, the putative fumiquinazoline gene cluster contains a stand-alone, monomodular NRPS predicted to activate L-Ala (Af12050, domain structure A-T-C) and also a predicted flavin adenine dinucleotide-dependent monooxygenase (Af12060) (Figure 1). While acylation of the indole NH group with L-Ala could occur before indole oxidation (*28*), we demonstrate in this work that oxidation of the indole 2′,3′-olefin by Af12060 is required prior to alanine coupling by Af12050 in a manner unprecedented for NRPS-based logic. This oxidative coupling strategy diversifies and expands multicyclic scaffolds, and we hypothesize that similar biosynthetic logic is likely involved in the formation a number of fungal indole alkaloids (Figure 2).

EXPERIMENTAL PROCEDURES

Materials and General Methods. Triphenyl phosphite, anhydrous pyridine, and anthranilic acid were purchased from Sigma-Aldrich. *N*-Boc-L-Ala-OH and *N*-Boc-Gly-OH were purchased from EMD Chemicals. D-Trp methyl ester hydrochloride was purchased from Toronto Research Chemicals. L-[U-^{14}C]Ala (128 mCi/mmol) was from Sigma-Aldrich, [1-^{14}C]acetyl-CoA[1] (60 mCi/mmol) from Moravek Biochemicals, and [^{32}P]PP$_i$ (100 mCi/mmol) from Perkin-Elmer. PCRs were conducted using Phusion High-Fidelity PCR MasterMix (New England Biolabs). Oligonucleotide primers were purchased from Integrated DNA Technologies (Coralville, IA). Plasmid DNA was propagated in *Escherichia coli* XL1 Blue (Stratagene), and plasmid DNA was

[1]Abbreviations: CoA, coenzyme A; cpm, counts per minute; EDTA, ethylenediaminetetraacetic acid; ESI, electrospray ionization; FAD, flavin adenine dinucleotide; HPLC, high-performance liquid chromatography; IPTG, isopropyl β-D-galactopyranoside; LC−MS, liquid chromatography−mass spectrometry; LB, Luria-Bertani medium; MeCN, acetonitrile; NAD(P)H, reduced nicotinamide adenine dinucleotide (phosphate); NCBI, National Center for Biotechnology Information; NMR, nuclear magnetic resonance; ORF, open reading frame; PDB, Protein Data Bank; PCR, polymerase chain reaction; PP$_i$, inorganic pyrophosphate; SDS−PAGE, sodium dodecyl sulfate−polyacrylamide gel electrophoresis; TCA, trichloroacetic acid; TCEP, tris(2-carboxyethyl)phosphine; Tris, tris(hydroxymethyl)aminomethane.

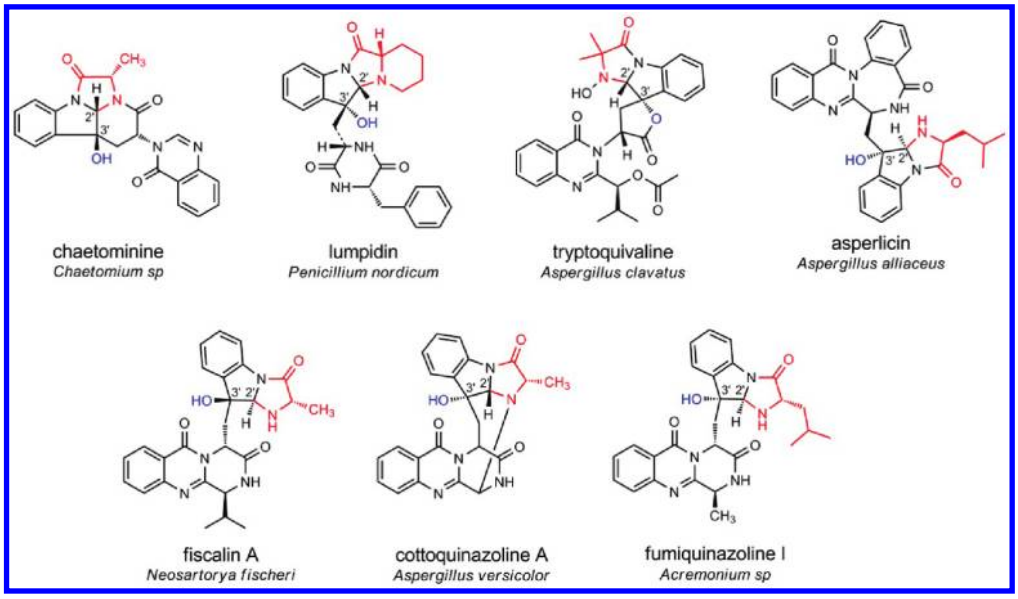

FIGURE 2: Examples of fungal metabolites containing a multicyclic indolic scaffold likely derived in part or in whole from an oxidative coupling transformation of indole with an additional amino acid in a manner similar to the generation of the imidazoindolone moiety of fumiquinazoline A. The indolic C2′ and C3′ positions are labeled for the sake of clarity.

prepared using the QIAprep Spin Mini Kit (Qiagen). Automated DNA sequencing was performed by Genewiz (South Plainfield, NJ). Protein concentrations were determined spectrophotometrically using measured A_{280} values and theoretical extinction coefficients obtained from the online ProtParam tool (*29*) (Af12050/pET30 Ek-LIC, ε = 120780 M^{-1} cm^{-1}; Af12060/pET30 Ek-LIC, ε = 91250 M^{-1} cm^{-1}). The concentrations of FQF and FQA were determined using UV−vis spectroscopy and published extinction coefficients of 13489 (277 nm) and 14791 M^{-1} cm^{-1} (256 nm), respectively (*5*). FQF, FQA, and GAT stock solutions (5 mM) were made with 50% DMSO in water. An Agilent Technologies 6520 Accurate-Mass QTOF instrument was used for high-resolution LC−MS analysis, an Agilent Technologies G1956 LC-MSD instrument for low-resolution analysis, and a Beckman Coulter System Gold instrument equipped with diode array detection for reverse-phase HPLC. Liquid scintillation counting was performed with a Beckman Coulter LS 6500 instrument. NMR data were collected on a Varian 600 MHz spectrometer using the residual solvent peak from incomplete deuteration as an internal standard ($CDCl_3$, δ 7.26).

Isolation and Characterization of FQF and FQA from an A. fumigatus Af293 Culture. An *A. fumigatus* Af293 spore stock (50 μL) was used to inoculate 50 mL of potato dextrose broth and the culture incubated at 37 °C for 24 h. Following growth, cells were removed by filtration (Whatman #54), the filtrate was applied to 5 mL of Amberlite XAD-16 resin (Sigma), and 2 × 5 mL volumes of MeOH were applied to elute absorbed compounds. The solvent was removed in vacuo and the resulting residue dissolved in 1.5 mL of MeOH (termed "XAD extract"). Solvent systems A (water with 0.1% formic acid) and B (MeCN with 0.1% formic acid) were used for LC−MS and HPLC analysis. For high-resolution LC−MS, 10 μL samples of XAD extract were injected onto a Gemini-NX C18 column (50 mm × 2.0 mm) and resolved with a gradient from 2 to 98% B over 12 min and a steady period of 98% B for 2 min with a flow rate of 0.4 mL/min. Under these conditions, FQA and FQF eluted with retention times of 8.3 and 8.6 min, respectively. For HPLC, 25 μL samples were injected onto an Alltima C18 column (150 mm × 4.6 mm) and resolved with a gradient from 5 to 95% B over 20 min and a steady period of 95% B for 5 min with a flow rate of 1 mL/min. Under these conditions, FQA and FQF eluted at 18.1 and 19.3 min, respectively.

Cloning of Af12060 and Af12050. Growth of *A. fumigatus* Af293, mRNA extraction, and cDNA preparation were performed as previously reported (*28*). The identification of a new 5′-start site for Af12060 was determined as described in Results. The start codon for this site is located at base 1700861 of the genomic DNA for Af293 chromosome 6 (GenBank accession number AAHF01000006.1), which is 210 bp upstream of the annotated start in AFUA_6g12060. Sequence alignment of results from a BlastP search indicated the presence of an intron in the newly added 5′-sequence and provided approximate intron boundaries. Manual inspection of the nucleotide sequence led to the identification of a 69 bp intron starting at base 1700701 (donor site) and ending at base 1700633 (acceptor site). PCR primers for amplification of Af12060 from cDNA were designed on the basis of this new start site and the annotated gene termination site: forward, 5′-GACGACGACAAGatgacaatcaacactgctctaccgactcc-3′; reverse, 5′-GAGGAGAAGCCCGG**tca**ctcgggactatatgtgtcctcc-3′ (lowercase type signifies bases complementary to the gene, and boldface type indicates the stop codon). The amplified DNA was cloned using a pET-30 Ek-LIC vector kit (EMD Chemicals), for expression as a 495-residue protein containing an N-terminal His_6-S tag. The boundaries of the new 5′-intron were confirmed by sequencing to be identical to that manually predicted. However, DNA sequencing revealed that the terminal 3′-intron (defined in the database as 21 bp, 1699627−1699605) was incorrectly predicted, with the correct 60 bp intron instead at bases 1699689−1699550.

Cloning of Af12050 also utilized a 5′-start site different from the annotated entry for ORF AFUA_6g12050 (as described in Results). This new start site begins at base 1695552 of the genomic DNA for Af293 chromosome 6, which is 582 nucleotides downstream of the start site of NCBI database entry NC_007199.1. PCR amplification of Af12050 from cDNA was accomplished using the following primer pair: forward, 5′-GACGACGACAAGatgttggagacgacggagccaattg-3′; reverse, 5′-GAGGAGAAGCCCGG**tca**caccgtaatctcagataacagagc-3′. The amplified DNA was

cloned into a pET-30 Ek-LIC vector to encode a 1153-residue protein with an N-terminal His_6-S tag, and the final construct was confirmed by DNA sequencing.

Expression and Purification of Af12050 and Af12060. Both protein constructs were overproduced in *E. coli* BL21-Gold(DE3) cells (Stratagene) in a similar manner. Cells (2 L) were grown at 37 °C in LB with 50 μg/mL kanamycin to an OD_{600} between 0.4 and 0.8, and the temperature was lowered to 16 °C prior to induction with 0.2 mM IPTG. Cells were harvested 18−24 h postinduction by centrifugation, suspended in lysis buffer [25 mM Tris-HCl (pH 7.5), 300 mM NaCl, 20% glycerol, 0.1% Tween 20, and 1× protease inhibitor cocktail (SigmaFast, EDTA-free)], and lysed using a EmulsiFlex-C5 homogenizer (Avestin). Insoluble material was removed by centrifugation (35000*g*) and the soluble protein applied to 1−2 mL of Ni-NTA agarose (Qiagen) equilibrated in lysis buffer. We performed Ni-affinity purification was performed by batch binding protein for 30 min at 4 °C, washing Ni resin with 2 × 20 mL of buffer A [50 mM Tris-HCl (pH 7.5) and 0.1 mM EDTA] containing 20 mM imidazole, and then eluting protein using a step gradient from 250 to 500 mM imidazole in buffer A (5 mL for each step). The elution fractions containing target protein were pooled and concentrated using a centrifugal filtration device (30K molecular weight cutoff, Amicon), and concentrated protein was flash-frozen in liquid N_2 and stored at −80 °C.

Synthesis and Characterization of Fumiquinazoline F (*FQF*) *and Glyantrypine* (*GAT*). The synthesis of FQF and GAT followed a previously described three-component one-pot microwave-assisted protocol (*30*). For the synthesis of FQF, anthranilic acid (140 mg, 200 μmol), *N*-Boc-L-Ala (190 mg, 200 μmol), and triphenyl phosphite (315 μL, 220 μmol) were combined with anhydrous pyridine (5 mL) in a round-bottom flask and heated in an oil bath for 16 h at 55 °C. After the sample had cooled to room temperature, D-Trp methyl ester hydrochloride (255 mg, 200 μmol) was added and the solution was divided among five septum-sealed 10 mL reaction vials and irradiated using a CEM Discover microwave reactor for 1.5 min at 220 °C. The resulting crude reaction mixture was concentrated in vacuo, and the residue was dissolved in CH_2Cl_2 and purified by silica gel flash chromatography (eluting with a 7:3:0.1 CH_2Cl_2/EtOAc/MeOH mixture). The desired fractions were concentrated, and the resulting residue was dissolved in 1 mL of DMSO for further purification using preparative reverse-phase HPLC, injecting 2 × 0.5 mL samples onto a Luna C18(2) column (250 mm × 21.2 mm) with a solvent system of water and acetonitrile, and running a linear gradient from 5 to 95% MeCN over 40 min at a flow rate of 8 mL/min. The peak corresponding to FQF and its enantiomer (t_R = 29 min) was collected, the MeCN removed in vacuo, and the remaining sample lyophilized. Acidic modifiers such as TFA and formic acid were avoided because of their contribution to epimerization at C3 of FQF. The correct enantiomer of FQF was determined using analytical chiral LC−MS (low-resoluton, Chiralcel OD-RH, 50 mm × 4.6 mm, 0 to 60% MeCN in water over 20 min, flow rate of 0.5 mL/min) with ESI+ mass detection by comparing the retention time of synthetic material with that of biologically derived FQF from the *A. fumigatus* XAD extract. The enantiomeric excess (ee) of FQF was determined to be 14% by analytical chiral HPLC (same column and gradient as described previously, flow rate of 1 mL/min); we prepared enantiopure FQF by injecting multiple samples of the scalemic mixture on the Chiralcel column and collecting the appropriate peak. Data supporting the identity of the synthetic FQF include high-resolution ESI/MS ($[M + H]^+$ expected, 359.1503; observed, 359.1492), UV−vis, and ^1H NMR data (*5*, *30*) (see Figures S5 and S6 of the Supporting Information).

GAT was synthesized using *N*-Boc-Gly (190 mg, 200 μmol) in place of *N*-Boc-L-Ala, and other components and methods as described for FQF. The crude reaction mixture was purified by silica-gel flash chromatography (solvent system as described for FQF) to yield GAT and its enantiomer. Data supporting the identity of the synthetic GAT include high-resolution ESI/MS ($[M + H]^+$ expected, 345.1346; observed, 345.1364), UV−vis, and ^1H NMR data (*30*) (see Figures S12C and S14 of the Supporting Information).

HPLC-Based Assays for Af12060. For determination of cofactor requirements, 50 μL reaction mixtures contained 5 μM Af12060 and 200 μM enantiopure FQF with or without 1 mM NADPH or NADH in NaP_i reaction buffer [50 mM sodium phosphate (pH 7.4), 100 mM NaCl, and 5% glycerol]. Reactions were initiated with enzyme, mixtures incubated at room temperature for 30−60 min, and then reactions quenched by addition of an equal volume of MeCN. Following incubation for an additional 5 min at 25 °C, the precipitant was removed by centrifugation, and 20 μL samples of the resulting supernatant were injected for HPLC analysis using an Alltima C18 column (150 mm × 4.6 mm), with detection at 274 nm. Solvent systems A (water with 0.1% formic acid) and B (MeCN with 0.1% formic acid) were used to apply a linear gradient from 0 to 60% B over 20 min, followed by a gradient from 60 to 95% B over 1 min, and a steady period of 95% B for 5 min with a flow rate of 1 mL/min. Under these conditions, a retention time of 21.9 min was observed for FQF, and retention times of 18.2 and 24.9 min were observed for products **3** and **4**, respectively.

For time course analysis of FQF utilization, a 350 μL reaction mixture was set up with 2 μM Af12060, 200 μM enantiopure FQF, and 1 mM NADPH in NaP_i reaction buffer. Reactions were initiated with enzyme and time points taken between 2.5 and 20 min by quenching 50 μL portions with an equal volume of MeCN. Quenched reactions were prepared for and analyzed by HPLC as described in the previous paragraph. FQF peak integration at 274 nm was used to generate a plot of FQF peak area versus time to approximate the enzymatic rate. Initial rate data, obtained as integration area per minute, were converted to micromolar per minute using a standard curve generated from 20 μL injections of FQF samples at a known concentration. Turnover was calculated on the basis of the enzyme concentration taking into account the fact that only ≈34% of the protein is in the holo and hence catalytically active form [turnover = rate/([enzyme] × 0.34)]. Additionally, both rate and turnover data were calculated by taking into account the concentrations of substrate and enzyme before the 2-fold dilution of the initial reaction volume from the MeCN quench.

ATP−[^{32}P]PP$_i$ Exchange Assay for Af12050. This assay was used to monitor the substrate-dependent exchange of the ^{32}P label of $[^{32}P]PP_i$ into ATP from the adenylation reaction catalyzed by the A domain of Af12050. Typical reaction mixtures (100 μL) contained 2 mM ATP, 2 mM $MgCl_2$, 3 mM $Na_4[^{32}P]PP_i$ (0.19 μCi), 5 μM Af12050, and 2 mM amino acid substrate in Tris reaction buffer [50 mM Tris-HCl (pH 7.5), 100 mM NaCl, 5 mM TCEP, and 5% glycerol]. Reactions were initiated by addition of enzyme, mixtures incubated at 25 °C for 1.5 h, and then reactions quenched by addition of a charcoal solution [1.6% (w/v) activated charcoal, 100 mM sodium pyrophosphate, and 3.5%

perchloric acid in water]. The charcoal was pelleted by centrifugation and washed with a solution containing 100 mM sodium pyrophosphate and 3.5% perchloric acid, and the charcoal-bound radioactivity was detected by liquid scintillation counting.

[^{14}C]Acetyl-CoA Labeling and [^{14}C]-L-Ala Loading Assays for Af12050. In vitro phosphopantetheinylation of Af12050 to generate holoprotein was monitored using radiolabeled acetyl-CoA and the phosphopantetheinyl transferase Sfp from *Bacillus subtilis* (*31*). A typical 400 μL reaction mixture contained 3 μM Af12050, 83 μM [1-^{14}C]acetyl-CoA (0.25 μCi), and 0.1 μM Sfp in Tris reaction buffer. Reactions were initiated by addition of Sfp and mixtures incubated at 25 °C for 1, 2.5, 5, 10, 20, or 45 min; at each time point, a 50 μL volume was quenched via addition to 0.5 mL of 10% TCA (with 50 μg of BSA for the visualization of the precipitated protein). Protein precipitate was pelleted by centrifugation, washed twice with 10% TCA, and dissolved in 80% formic acid for liquid scintillation counting. A ratio of nanomoles of radioactivity counted to nanomoles of protein was used to calculate the percent conversion based on 1 equiv of [1-^{14}C]acetyl-CoA labeling 1 equiv of Af12050.

The loading of radiolabeled L-Ala onto apo- or holo-Af12050 was performed to monitor the in cis thiolation activity of the A-T pair of Af12050. Apo-Af12050 was obtained by protein production in *E. coli* BL21-Gold(DE3) cells followed by Ni-affinity purification. Holoprotein was generated in vitro with the Ni-affinity-purified protein using CoA and Sfp (2 mM CoA, 1 mM $MgCl_2$, and 2 μM Sfp added directly to purified Af12050, incubation for 30 min at 25 °C). Then, a 400 μL reaction mixture was set up to contain 3 μM holo-Af12050, 5 mM ATP, and 50 μM L-[U-^{14}C]Ala (0.32 μCi) in Tris reaction buffer. For time point analysis, 50 μL volumes of the reaction mixture were quenched 0.5, 1, 2.5, 5, 10, 20, and 30 min after addition of [^{14}C]Ala substrate with 10% TCA, and the precipitated protein was collected and prepared for liquid scintillation counting as described in the previous paragraph. The percentage loading of [^{14}C]Ala was calculated as the mole fraction of ^{14}C-labeled substrate covalently transferred to holo-Af12050 protein assuming 1:1 stoichiometry.

Reconstitution of FQA Biosynthesis. To address the requirement for tethering of L-alanine as a pantetheinyl intermediate to the T domain of Af12050 for FQA production, 50 μL reaction mixtures were set up to contain 2.5 μM Af12060, 2 mM $MgCl_2$, 2 mM NADPH, 1 mM L-Ala, and 200 μM enantiopure FQF in NaP_i reacton buffer with varying combinations of 1 mM ATP and 5 μM apo- or holo-Af12050. (1) To address the ability of Af12050 to catalyze acylation of FQF with free L-Ala, apo-Af12050 was used without addition of ATP. (2) To address coupling of L-Ala-AMP to FQF by Af12050, the reaction mixture included ATP and apo-Af12050. (3) To reconstitute L-Ala-S-Enz formation (as tethered to the T domain of Af12050), the reaction mixture included ATP and holo-Af12050 (generated in vitro by preincubation of apo-Af12050 with CoA and Sfp). Reactions were initiated by addition of Af12060 and mixtures incubated for 40 min at 25 °C prior to quenching with 50 μL of MeCN. The precipitate was removed by centrifugation, and 20 μL of the clarified supernatant was injected onto an Alltima C18 column (150 mm × 4.6 mm) for HPLC analysis (274 nm detection). The injected sample was separated using a gradient from 0 to 60% MeCN over 20 min, a gradient from 60 to 95% MeCN over 1 min, and a steady period of 95% B for 5 min at a flow rate of 1 mL/min (solvent system of water and acetonitrile with 0.1% formic acid). Under these conditions, **3**, FQA, FQF, and **4** eluted at 18.2, 20.6, 21.9, and 24.8 min, respectively. Data supporting the identity of the enzymatically prepared FQA include high-resolution ESI/MS ([M + H]$^+$ expected, 446.1818; observed, 446.1823), UV−vis, and ^{1}H NMR data (*5*, *30*) (see Figures S10 and S11 of the Supporting Information).

A time course study was performed to obtain apparent rate data of FQF utilization and FQA formation by combining Af12050 and Af12060. A 250 μL reaction mixture was set up to contain 1 μM Af12060, 5 μM holo-Af12050, 1 mM NADPH, 1 mM ATP, 2 mM $MgCl_2$, 1 mM L-Ala, and 200 μM FQF in NaP_i reaction buffer. Aliquots (50 μL) were taken at 5, 10, 25, and 60 min after the addition of Af12060 (to initiate reaction) and reactions quenched with an equal volume of MeCN. Samples (20 μL) were prepared for and analyzed by HPLC as described in the previous paragraph. FQF and FQA peak integration and initial velocity estimates were determined as described in HPLC-Based Assays for Af12060 using FQF and FQA standards (concentrations calculated using published extinction coefficients as described in Materials and General Methods).

Spectrophotometric Assay for Substrate-Dependent NADPH Consumption by Af12060 with or without Af12050. For the assay of Af12060 alone, 200 μL reaction mixtures contained 1 μM Af12060, 200 μM NADPH, and varying concentrations of FQF (5−200 μM) in NaP_i reaction buffer. For the assay of Af12060 in the presence of Af12050, 200 μL reaction mixtures contained 1 μM Af12060, 5 μM holo-Af12050, 200 μM NADPH, 1 mM ATP, 1 mM L-Ala, 2 mM $MgCl_2$, and varying concentrations of FQF (5−200 μM) in NaP_i reaction buffer. Holo-Af12050 was generated in vitro using Sfp and CoA prior to addition. Reactions were initiated by addition of Af12060 and continuous spectrophotometric data collected at 340 nm (on a Varian Cary 50 Bio instrument) in triplicate for each concentration of FQF. Initial rate data (in absorbance units per minute) representing NADPH consumption were converted to micromolar per minute using the extinction coefficient for NADPH of 6200 M^{-1} cm^{-1}. In the absence of substrate, and consistent with observation from HPLC-based assays, oxidation of NADPH by holo-Af12060 did not occur to any appreciable degree unless excess FAD was included in the reaction mixture. Utilization of NADH in place of NADPH provided similar rate data, and including the (3*R*,14*S*) enantiomer of FQF did not decrease the measured rate.

Biosynthesis of FQA Analogues. For biosynthesis of FQA analogue 1 [**7** (Figure S12 of the Supporting Information)], a 100 μL reaction mixture consisted of 2 μM Af12060, 4 μM holo-Af12050, 1 mM NADPH, 1 mM ATP, 2 mM $MgCl_2$, 1 mM L-Ala, and 100 μM GAT in NaP_i reaction buffer. After 2 h at 25 °C, the reaction was quenched by addition of 100 μL of MeCN and a 10 μL sample was analyzed by high-resolution LC−MS [Gemini-NX C18 column, 150 mm × 4.6 mm, 2 to 98% MeCN in water (0.1% formic acid) over 13 min at a flow rate of 0.4 mL/min]. Under these conditions, the retention times of **7** and GAT were 9.7 and 10.2 min, respectively. A similar experimental design was used to monitor biosynthesis of FQA analogue 2 [**8** (Figure S13 of the Supporting Information)], but the reaction mixture included 100 μM FQF (instead of GAT) and 1 mM glycine (instead of L-Ala). Under the LC−MS conditions described for **7**, analogue **8** eluted at a retention time of 9.8 min.

RESULTS

Identification of Fumiquinazolines F and A from an A. fumigatus Af293 Culture. Although the production of FQF

and FQA from *A. fumigatus* Af293 has been previously reported (*6*), our own identification of these compounds from Af293 culture broth extracts proved to be useful in the characterization of synthetic FQF and the enzymatic reconstitution product FQA. A culture broth extract, prepared following growth of *A. fumigatus* Af293 for 24 h at 37 °C in potato dextrose broth, was analyzed by high-resolution LC−MS and analytical HPLC (Figure S2 of the Supporting Information). Mass filtering of the total ion current chromatogram identified FQA ($[M + H]^+$ expected, 446.1823; observed, 446.1812) and FQF ($[M + H]^+$ expected, 359.1503; observed, 359.1495) as two of the seven most prominent peaks detected. Support for the positive identification of these two peaks as FQA and FQF was provided by matching the UV−vis spectra from diode array detection with previously published data (*5*).

Cloning, Expression, and Purification of Af12050 and Af12060. Genes encoding Af12050 and Af12060 were cloned from *A. fumigatus* Af293 cDNA using start sites that varied from the ORF annotations found in the NCBI database. The alternate start sites were determined on the basis of multiple-sequence alignment generated via BlastP and by analysis of homology models generated using HHpred (*32*). For Af12060, sequence alignment suggested that the ORF as annotated (AFUA_6g12060, GenBank accession number XM_745992.1) would encode a truncated version of the protein lacking ≈50 residues at the N-terminus. Modeling based on PDB entry 2RGJ suggested that these additional residues are necessary to form two β-strands and an α-helix that are critical for interaction with the adenosine pyrophosphate of FAD. Inspection of the 5′-sequence upstream of the annotated start site led to the identification of an additional exon−intron pair that was used as the basis for designing the forward primer for PCR amplification. For Af12050, an alternate start site was identified following failed attempts to clone the gene from cDNA using primers designed for the start site of NCBI database entry AFUA_6g12050 (GenBank accession number XM_745991.1). The new start site identified and utilized for cloning is 582 nucleotides (mature transcript coding for 49 amino acids) downstream of the start codon of AFUA_6g12050, eliminating the first exon−intron pair of the database entry. The alternate start site for Af12050 is in agreement with the majority of the top 100 hits returned from BlastP and is suggested to encode a structurally complete A domain (as part of the full-length A-T-C protein) based on homology modeling. Both Af12060 and Af12050 were cloned into pET30 Ek-LIC vectors to encode N-terminal His_6-S tag proteins (Af12050, 128 kDa; Af12060, 55 kDa), expressed using *E. coli* BL21-Gold(DE3), and purified by Ni-affinity chromatography (Figure S3 of the Supporting Information). Af12060 was purified as a bright yellow protein to >90% purity with a yield of 32 mg/L, while Af12050 eluted from the Ni resin in moderate yield (12 mg/L) with a purity of ≈60%, likely due to contamination by degraded and/or truncated versions of the target protein.

Characterization of Af12060. Gene annotation and sequence analysis suggested that Af12060 is a FAD-dependent oxidoreductase. Homology modeling provided additional insight, suggesting that Af12060 is a class A monooxygenase that contains noncovalent but tightly bound FAD, requires NAD(P)H as a coenzyme, and should possess an overall structure (for residues 1−420) similar to that of the aromatic hyroxylase PhzS from *Pseudomonas aeruginosa* (*33*, *34*). The UV−vis spectrum of purified Af12060 supported the presence of bound flavin cofactor (Figure S4A,B of the Supporting Information). The identity of the flavin cofactor as FAD was further confirmed by HPLC analysis of the supernatant from heat-denatured Af12060 (Figure S4C of the Supporting Information). The percent holoprotein was determined to be 23% for the native enzyme using absorbance values specific for protein (A_{280}) and flavin (A_{446}) or 34% when using the A_{446} of the released FAD following protein denaturation (Figure S4A,B of the Supporting Information). The discrepancy in percent holo-Af12060 may arise from quenching of the FAD A_{446} signal when bound to enzyme.

Fumiquinazoline F, a candidate substrate for Af12060, was chemically synthesized from anthranilic acid, *N*-Boc-L-alanine, and D-tryptophan methyl ester hydrochloride using a modified literature procedure (*30*). Enantiopure FQF was purified from the crude reaction mixture by sequential silica gel flash chromatography, semipreparative reverse-phase HPLC, and chiral-phase HPLC (Figure S5A of the Supporting Information). The identity of FQF was further supported by MS, UV−vis, and NMR spectroscopy (Figures S5B and S6 of the Supporting Information).

Incubation of enantiopure FQF with purified Af12060 and reduced nicotinamide cofactor (NADPH or NADH) led to the disappearance of FQF and the formation of two new products (**3** and **4**) in an enzyme- and time-dependent manner (Figure 3A,B). By monitoring the disappearance of FQF over time, we obtained an apparent reaction velocity of 11 μM min^{-1} and turnover number of 16 min^{-1} for the experimental conditions assayed (2 μM Af12060, 200 μM FQF, and 1 mM NADPH). Further kinetic analysis of Af12060 was hampered because of substrate inhibition (Figure S7 of the Supporting Information). The UV−vis spectra of **3** and **4** are similar to those obtained for FQF, but there are notable differences in the range of 275−290 nm, suggesting possible modification of the indole moiety of FQF (Figures S8 and S9 of the Supporting Information). Although the instability of compounds **3** and **4** hindered structural identification by NMR spectroscopy, mass spectral analysis suggested that **3** is a dihydroxylated version of FQF (FQF-indoline-2′,3′-diol, $[M + Na]^+$ expected, 415.1386; observed, 415.1386) and that **4** is an oxidized dimer ($[M + H]^+$ expected, 749.2831; observed, 749.2845) (Figures S8 and S9 of the Supporting Information).

The biosynthetic intermediate leading to the formation of either **3** or **4** is postulated to be an indole C3′-hydroxyiminium species (**1**) or a 2′,3′-epoxyindole (**2**) generated by the enzymatic oxidation of FQF by Af12060 (Figure 3C). As an FAD- and NAD(P)H-dependent monooxygenase, we postulate that Af12060 catalyzes the reduction of FAD to $FADH^-$, which reacts with molecular oxygen to form a C4a-peroxyflavin species that is then protonated to yield C4a-hydroperoxyflavin. The 2′,3′-double bond of the pendant indole could serve as the nucleophile for capturing the electrophilic hydroxyl group of the hydroperoxyflavin to generate **1**. Epoxide formation to form **2** may then occur via intramolecular capture by the 3′-OH group. In the absence of downstream enzymatic machinery, and on the basis of the electrophilic reactivity at indole-derived C2′ of the oxy-FQF intermediate, release of **1** or **2** from the enzyme active site could lead to capture by water from bulk solvent to yield **3**, or dimerization to form some variety of **4**. Additional details regarding characterization of **3**, including isotope labeling studies using $[^{18}O]H_2O$, are provided as Supporting Information.

Characterization of Af12050 and Reconstitution of FQA Biosynthesis. Af12050 is a monomodular three-domain (A-T-C) NRPS that we predict to selectively activate and couple L-alanine

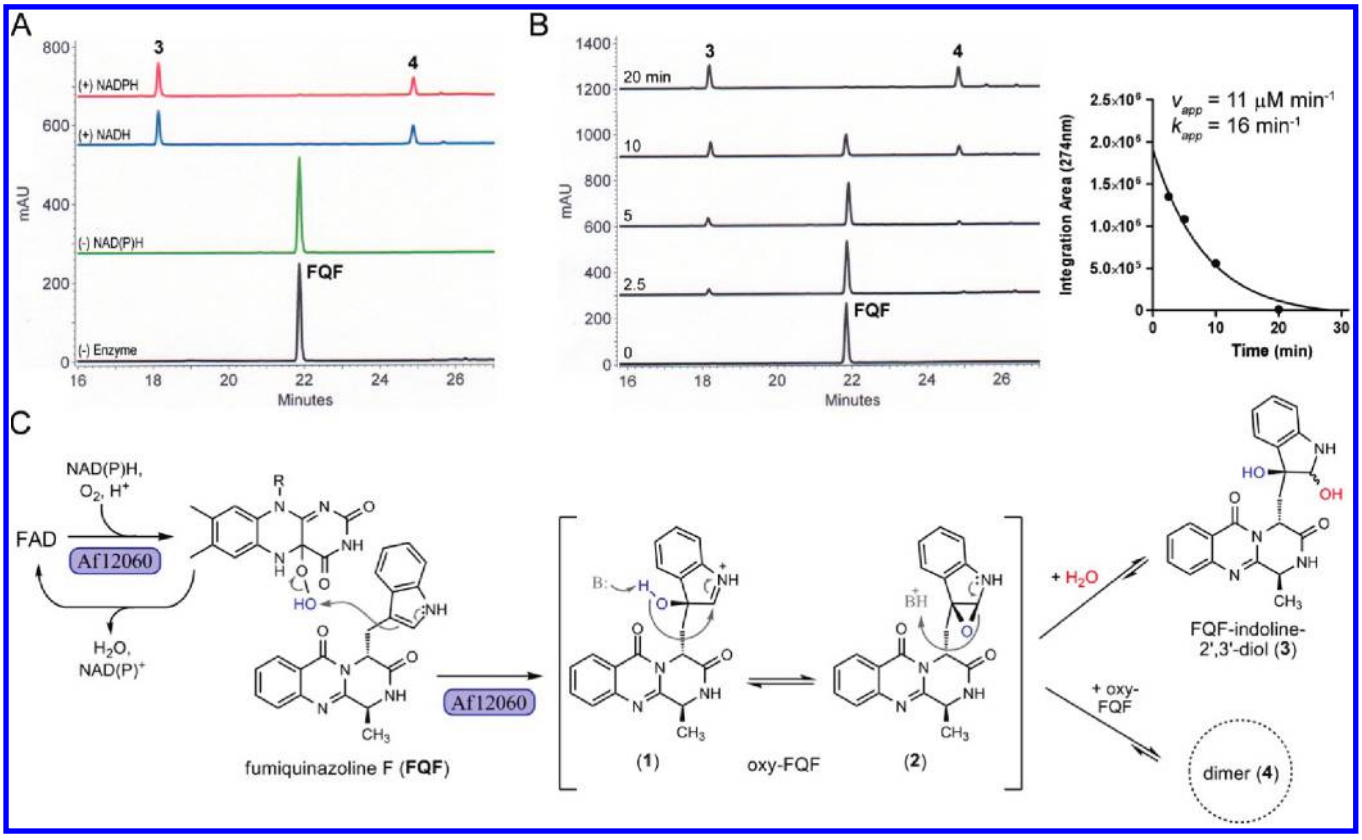

FIGURE 3: Biochemical characterization and proposed mechanism of the FAD- and NAD(P)H-dependent monooxygenase, Af12060. (A) HPLC analysis (274 nm detection) of reaction mixtures containing 200 μM FQF and 5 μM Af12060 with or without 1 mM NADPH or NADH. Reactions were quenched after incubation for 40 min at 25 °C via addition of 50% MeCN. (B) Time course for FQF utilization and accompanying rate data obtained by integration of the FQF peak area. The reaction mixture contained 200 μM FQF, 2 μM Af12060, and 1 mM NADPH; reactions were quenched at the indicated time point by addition of MeCN. (C) Proposed pathway for the conversion of FQF to **2** and **3** by Af12060. Brackets denote putative intermediates not detected by HPLC or LC−MS analysis. Possible structures for the oxidized dimer species (**4**) are provided in Figure S9A of the Supporting Information.

to the oxidized indole of FQF. The putative 10-residue substrate specificity sequence for the A domain of Af12050 is 80% similar to the L-Ala-specific A domain from module 11 of cyclosporin A synthethase (*35*, *36*). Experimental validation of Ala-specific adenylation and thiolation activity was accomplished using full-length protein, with the apo form obtained as purified from *E. coli* and the holo form generated in vitro by incubation with CoA and the phosphopantetheinyl transferase Sfp (*31*) (Figure 4A).

The amino acid preference for adenylation by Af12050 was investigated by monitoring the substrate-dependent exchange of radioactive [^{32}P]PP$_i$ into ATP. As illustrated in Figure 4B, L-Ala is the preferred substrate for adenylation by the A domain of apo-Af12050, while Gly, L-Ser, D-Ala, and L-Val also promote exchange above the background level (20, 10, 7, and 4% of the level observed for L-Ala, respectively). Conversion of the Af12050 T domain from apo to holo was assayed by incubation with Sfp and [^{14}C]acetyl-CoA to achieve ≈22% conversion to the acetyl-S-pantetheinylated holo form. Transfer of the alanyl group of the activated L-Ala-AMP to the holo T domain as an aminoacyl thioester was assayed using [^{14}C]-L-Ala (Figure 4C). A maximal loading of 24% [^{14}C]-L-Ala was reached between 5 and 10 min after initiation of the reaction. When Sfp was omitted from the reaction mixture, no labeling of Af12050 with [^{14}C]-L-Ala was observed, demonstrating that Af12050 purified from *E. coli* is in apo form.

The ability of Af12050 to selectively activate and load L-Ala set the stage for evaluation of the ability of this same enzyme to couple an enzyme-tethered alanine to the indole-derived side chain of oxy-FQF to reconstitute FQA biosynthesis. Evidence that FQF is not a direct substrate for Af12050 is provided in Figure 5A (bottom two traces); incubation of holo-Af12050, L-Ala, Mg^{2+}, ATP, and FQF does not lead to a decrease in the level of FQF or to the formation of any new peaks that could represent alanyl-FQF intermediates. The requirement for an alanyl-S-Enz intermediate for productive coupling of Ala to oxy-FQF was investigated using apo- or holo-Af12050, Af12060, NADPH, Mg^{2+}, and L-Ala with or without ATP (Figure 5A, top three traces). The different combinations tested illustrate that (1) free L-Ala is not a substrate for coupling (middle trace, products **3** and **4**), (2) L-Ala-AMP is not a substrate for coupling (second trace from the top, products **3** and **4**), and (3) including Af12060 and holo-Af12050 with the necessary components for FQF oxidation and alanyl-S-Enz formation leads to the production of a single new product identified as **FQA** [top trace; $[M + H]^+$ expected, 446.1823; observed, 446.1818 (see Figures S10 and S11 of the Supporting Information)]. A time course study monitoring the conversion of FQF to FQA by analytical HPLC did not detect intermediate compounds or the presumed shunt metabolites **3** and **4** (Figure 5B). The putative intermediates for this reaction are likely short-lived and therefore not detected, but the absence of detectable amounts of **3** and **4** suggests that (1) if formed, **3** and **4** are in equilibrium with the predicted on-pathway intermediates [e.g., **1** and **2** (Figure 3C)] and/or (2) Af12060 and Af12050 are a highly efficient pair for the net oxidative acylation of FQF to form FQA. Intermediate channeling between an enzyme complex

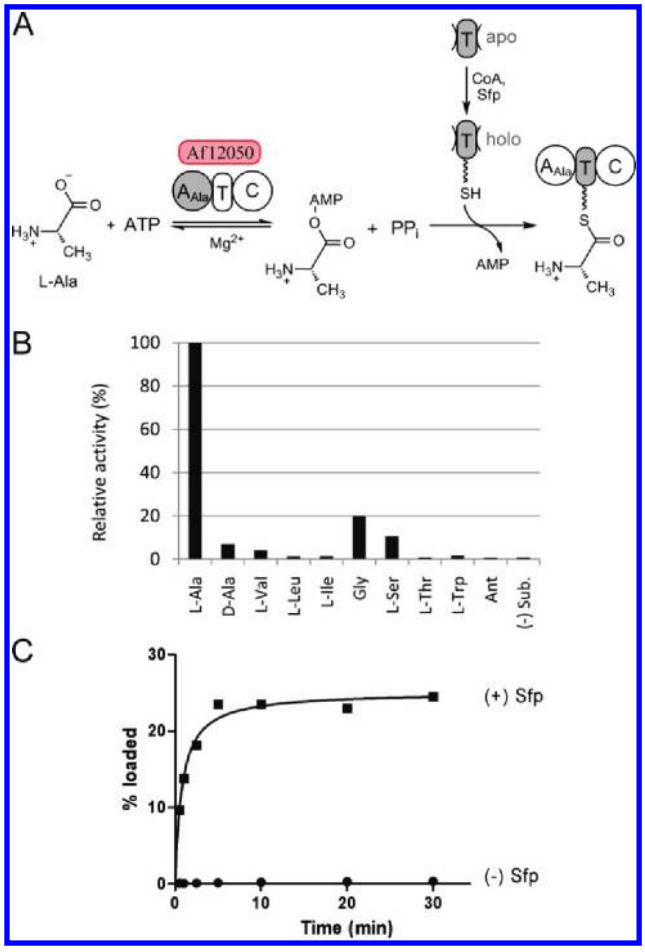

FIGURE 4: Characterization of substrate-dependent adenylation activity and L-Ala loading of Af12050. (A) Schematic for the two-step process of adenylation (to generate an activated L-alanyl-AMP intermediate) and subsequent loading of the L-alanyl group onto the 4′-phosphopantatheine group of the holoprotein. (B) ATP–[^{32}P]PP$_i$ exchange activity promoted by apo-Af12050 with various amino acids tested as substrates (100% activity corresponds to 112000 cpm). Reactions were quenched with activated charcoal following a 1.5 h incubation at 25 °C, and radioactivity was detected by liquid scintillation counting. (C) Time course for the loading of radiolabeled [^{14}C]-L-Ala onto Af12050 protein that was purified directly from *E. coli* BL21(DE3) cells (●, apoprotein) or following in vitro incubation with *B. subtilus* Sfp and CoA for T domain phosphopantetheinylation (■, holoprotein).

of Af12060 and Af12050 is one possible means of achieving efficient product formation without off-pathway capture of the reactive intermediate by water or through dimerization; however, gel filtration chromatography did not detect formation of a protein complex. Apparent rates associated with the conversion of FQF to FQA were estimated using the data from the HPLC time course experiment (right panel of Figure 5B); as anticipated for efficient product formation, the apparent initial velocity of FQF disappearance (4.0 μM min^{-1}) matches the rate of FQA appearance (3.8 μM min^{-1}).

We propose two alternative pathways for the enzymatic conversion of FQF to FQA by Af12060 and Af12050 (Figure 5C). Activation and loading of L-Ala by Af12050 primes this enzyme for coupling of alanine to oxy-FQF, where oxidation of the indole 2′,3′-double bond of FQF is catalyzed by Af12060 via 2′,3′-epoxidation (**2**) or 3′-hydroxylation (**1**) (Figure 3C). Subsequently, and consistent with the role of C domains in the chemistry of N–C bond formation (*37*), we anticipate that the terminal C domain of Af12050 binds both the free oxy-FQF intermediate (**1** or **2**) and the T domain-tethered, L-Ala-S-Enz intermediate, to bring these two species into proximity for reaction. For pathway A, the indoline NH group of intermediate **2** could serve as the nucleophile for attack at the thioester carbonyl of the enzyme-tethered L-Ala. The net result would be N-acylation of the epoxyindoline via amide bond formation and release of the L-alanyl intermediate from Af12050. Subsequently, activation of the alanyl-α-amino group of intermediate **5** by the C domain and attack at indoline C2′ would result in the favorable 5-exo-tet intramolecular cyclization that is concomitant with epoxide ring opening. For pathway A, the stereochemistry of the epoxide (as installed by Af12060) would dictate the observed trans stereochemistry at positions C3′ and C2′ of the resulting imidazoindolone by necessitating an S_N2-mediated attack of the alanyl NH_2 group at C2′. For pathway B, position C2′ of the indole-derived 3′-hydroxyiminium (**1**) serves as the electrophilic center for attack by the C domain-activated α-amino group of the alanyl-S-Enz intermediate. At this point, the alanyl-oxy-FQF intermediate (**6**) would remain tethered to the T domain of Af12050, with chain release and the favorable intramolecular 5-exo-trig ring closure occurring by attack of the indoline NH group on the thioester carbonyl. This reaction may occur in the active site of the C domain but may also be spontaneous. For path B, the final stereochemistry at positions C2′ and C3′ of the indoline could be influenced in part by the stereochemistry of the hydroxylation step and/or the direction of attack by the alanyl-α-amino group as dictated by the C domain active site architecture.

Substrate Tolerance of Af12060 and Af12050 and Biosynthesis of FQA Analogues. The monooxygenase Af12060 is sensitive to changes in the stereochemistry of FQF at C14 (functionality derived from D-Trp) but not at position C3 (from L-Ala); the enantiomer of FQF, with a (3*R*,14*S*) configuration, is not a substrate for Af12060, while FQG, a diastereomer with a (3*R*,14*R*) configuration, is a substrate (data not shown). Additionally, assays using a mixture of synthetic FQF with its enantiomer (in a 57:43 ratio) with Af12060 (with or without Af12050) did not result in altered production of **3**, **4**, or FQA or hinder the rate of product formation, suggesting that the enantiomer of FQF is not an inhibitor.

To further explore substrate tolerance as well as the potential utility of applying the two enzymes Af12060 and Af12050 in tandem to generate molecules with a 6-5-5 muticyclic imidazoindolone scaffold, we reconstituted the production of two FQA analogues: **7** (Figure S12 of the Supporting Information) and **8** (Figure S13 of the Supporting Information). Compound **7** arises from the enzymatic processing of glyantrypine (GAT) (*11*). The only difference between FQF and GAT is the change in functionality at position C3 of the pyrazinoquinazolinone tricycle; FQF contains a methyl substituent derived from L-Ala, while GAT lacks functionality at this position because of incorporation of Gly. GAT was synthesized in a manner similar to that of FQF and obtained as a mixture of enantiomers. Upon combining the holo versions of both Af12060 and Af12050 in a reaction mixture containing NADPH, ATP, and L-Ala with synthetic GAT, the formation of **7** was detected by LC–MS (Figure S12 of the Supporting Information). The production of **7** indicates that a methyl substituent at C3 is not essential for substrate recognition or productive binding by either Af12060 or Af12050. On the basis of the exclusive preference of Af12060 for (3*S*,14*R*) FQF over the (3*R*,14*S*) FQF enantiomer, we presume

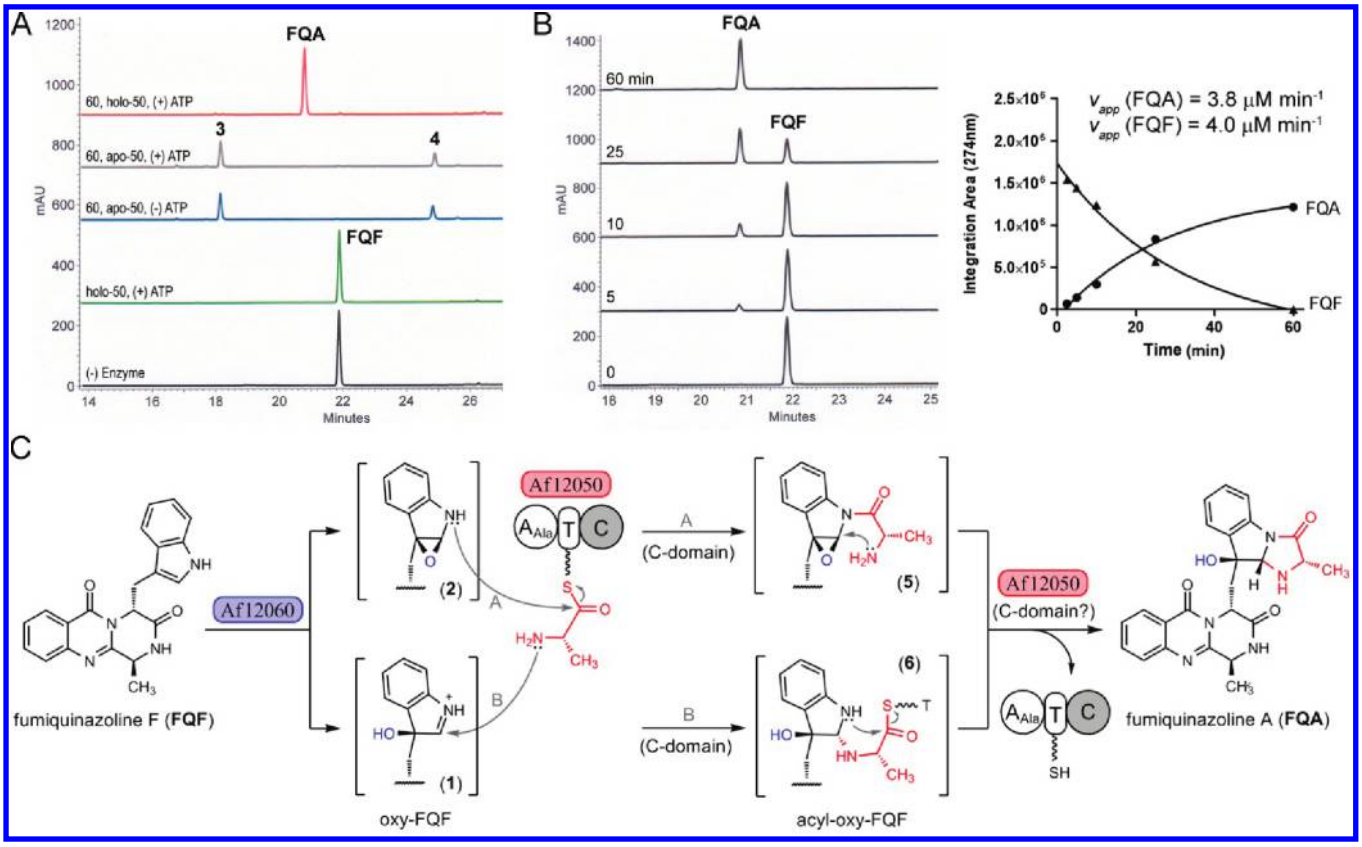

FIGURE 5: Reconstitution of fumiquinazoline A (FQA) biosynthesis by combining Af12060 (monooxygenase) and Af12050 (nonribosomal peptide synthetase) with FQF as the substrate. (A) HPLC analysis of reaction mixtures containing 200 μM FQF, 1 mM NADPH, 1 mM L-Ala, 2 mM Mg^{2+}, and various combinations of 2.5 μM Af12060 (abbreviated as 60), 5 μM Af12050 (abbreviated as 50), and 1 mM ATP. The (−) enzyme control contained all reaction components except Af12050 and Af12060. Holo-50 denotes phosphopantetheinylated protein. (B) Time course of FQA production and accompanying rate data for FQF utilization and FQA formation. The concentrations of components used were the same as those for panel A, except for 1 μM Af12060. (C) Two proposed pathways for the conversion of FQF to FQA by Af12060 and Af12050. Brackets denote putative intermediates not detected by HPLC or LC−MS analysis. The C domain of Af12050 is postulated to catalyze the two-step process of L-Ala coupling and subsequent intramolecular attack to generate the 6-5-5 imidazoindolone moiety of FQA.

that the stereochemistry of **7** is (14*R*). Additionally, though L-Ala is the preferred substrate for adenylation by Af12050, Gly is also activated and promotes a level of exchange that is ≈20% that of L-Ala (Figure 4B). To investigate the ability of Af12050 to activate, load, and couple Gly to oxy-FQF, holoenzymes Af12060 and Af12050 were combined with NADPH, ATP, FQF, and Gly, and product analysis was performed by LC−MS (Figure S13 of the Supporting Information). A small amount of the glycine-derived product **8** was observed, while the majority of the product formed was the indoline-2′,3′-diol (**3**). These results suggest that the coupling of glycine to the N1′ and C2′ positions of the oxidized indole of FQF occurs; however, this process is much less efficient than when L-Ala is used as a substrate for Af12050 and leads to the formation of the uncoupled product **3**.

DISCUSSION

Oxidation of FQF by Af12060. This study indicates that Af12060 is a single-component FAD-dependent monooxygenase that acts on the pendant indole side chain of FQF. We propose a mechanism that involves hydroxylation at C3′ of the indole moiety (**1**) and possible conversion to a 2′,3′-epoxyindole (**2**) (Figure 3C). The initial hydroxylation of FQF by Af12060 may be similar to flavoprotein-catalyzed hydroxylation of phenolic compounds, where a C4a-hydroperoxy-FAD is the electrophilic oxygenating species for a nucleophilic substrate (*38*). In analogy to the hydroxyl activating substituent of phenolic compounds (e.g., 4-OH-benzoate) that can generate an adjacent carbanion equivalent, hydroxylation of the pendant indole of FQF may involve participation of the pyrrole NH group. Conversion of **1** to the epoxy intermediate **2** may not necessarily occur; however, the formation of **2** prior to alanine coupling and intramolecular cyclization could control the observed stereochemistry of the imidazoindolone scaffold of FQA. One possible precedent is epoxidation of the terminal olefin of squalene by the two-component FAD-dependent squalene epoxidase, proposed to catalyze donation of electrophilic oxygen from hydroperoxy-flavin for hydroxylation followed by intramolecular capture to form an epoxide product (*39*). For Af12060, we note that interconversion of **1** and **2** may occur in the enzyme active site.

Oxidation of the pyrrole ring of indoles by non-heme iron or cytochrome-type oxgenases has been reported previously (*40*, *41*), including the degradation of L-Trp to *N*-formylkynurenine by two heme/O_2-dependent dioxygenases (*42*). Additionally, the 2′,3′-epoxidation of indole by the P450 monooxygenase KtzM is postulated to occur in the biosynthesis of the kutzneride building block dichlorohydroxyhexahydropyrrole indole (*43*). However, reports describing the flavin-dependent oxidation of indole are much less common. Hydroxylation at indole C2 or C3 leading to indigo and indirubin has been reported for an engineered variant of the class A flavoprotein 2-hydroxybiphenyl 3-monooxygenase, HbpA (*44*) (15% identical and 48% similar to Af12060 for residues 1−452). The hydroxyindole reaction products produced by HbpA are reported to be unstable and spontaneously

oxidize and dimerize to form pigments (*44*). Analogously, the presumed oxy-FQF intermediates **1** and **2** were not isolated during the course of experimentation; rather, the compounds isolated were from spontaneous reaction with water (**3**) or dimerization (**4**). With regard to modification of a pendant indole group as part of a more complex natural product, the oxidation at indole C2 of a bisindolepyrrolidone by VioC has been reported in the biosynthesis of violacein (*45*). VioC and Af12060 are class A flavoprotein monooxygenases that share moderate amino acid sequence homology (16% identical and 50% similar). Additionally, the flavoprotein oxidation of a Trp-derived indole via 2′,3′-epoxidation has been proposed for the biosynthetic route to the natural products notoamides C and D (*46*) [the recently reported gene cluster contains two Af12060 homologous, NotB and NotI (*47*)]. The characterization of Af12060 provides an intriguing example of flavoprotein-catalyzed oxidation of indole and expands upon the small number of known or proposed flavin-dependent monooxygenases that modify the C2 or C3 position of indole or indole-derived metabolites.

Enzymatic Conversion of FQF to FQA. The FAD- and NAD(P)H-dependent monooxygenase Af12060 and the alanine-activating tridomain NRPS Af12050 are necessary and sufficient to convert FQF to FQA, an enzymatic process requiring tailoring of a Trp-derived indole via oxidation and dual N−C bond formation to form a 6-5-5 imidazoindolone ring system. Initially, the order of oxidation and alanine coupling was unknown. We had previously proposed N-acylation of FQF via nucleophilic attack of the indole NH group of FQF on an activated alanyl-S-Enz thioester, and then oxidation of the indole 2′,3′-olefin and intramolecular attack of the alanine α-amino group on C2′ of the *N*-acylindole (*28*). However, the ability of Af12060 to accept FQF as a substrate and the observation that incubation of L-alanyl-S-Af12050 with FQF did not result in the formation of any new products suggested that the order of enzymatic events actually starts with indole oxidation by Af12060 followed by acylation with L-Ala and cyclization by Af12050. While this order may be dictated to some degree by enzyme substrate specificity, perhaps a more important consideration is the reactivity of the substrate, with oxidation of the indole 2′,3′-olefin activating the indole-derived functionality for N-acylation.

With regard to the timing of indole N-acylation, parallels may be drawn between the N-alanylation of oxy-FQF (Figure 5C) and the N-acetylation of aszonalenin (*48*) (Figure S15 of the Supporting Information), based on the transformation process and associated reactivity of the Trp-derived indole. In both cases, the aromaticity of the pyrrole portion of indole is lost prior to N-acylation due to modification at indole C3. For azonalenin, there is prenylation by AnaPT at C3 coupled to intramolecular cyclization (N12 of the benzodiazepine attacks the indole C2). The indole-derived nitrogen of the resulting compound (aszonalenin) is an aniline-like secondary amine, which is now presumed to be sufficiently nucleophilic for attack on the thioester carbonyl of acetyl-CoA to yield the N-acetylated product acetylaszonalenin. For the conversion of FQF to FQA, the oxidation at indole C3′ by Af12060 (either as the 3-hydroxyiminium or the 2′,3′-epoxide) occurs prior to the coupling of L-alanine by Af12050 via two consecutive N−C bond formations. For path B of Figure 5C, the oxidation at indole C3′ of FQF (similar to prenylation at indole C3 of the benzodiazepinedione) abolishes aromaticity and results in generation of a positively charged iminium species that renders the indole C2 electrophilic and susceptible to nucleophilic attack. For path A of Figure 5C, epoxidation serves a purpose similar to that of prenylation in abolishing indole aromaticity, but in the case of epoxidation, there is an oxygen neighboring the indole NH group resulting in hemiaminal functionality. Because FQF is not a substrate for Af12050, we hypothesize that if path A is operant, the epoxidation likely enhances the nucleophilicity of the indole NH group due to rehybridization of C2′ and C3′ from sp^2 to sp^3 and/or the formation of the epoxide is a critical recognition determinant for L-Ala coupling by Af12050.

Acylation of oxy-FQF by Af12050 represents the first characterized example of nonribosomal peptide synthetase-based coupling of an amino acid to the pyrrole ring of indole. We propose that the coupling step may be catalyzed by the terminal C domain of Af12050 that would bind in cis a T domain-tethered alanyl-S-pantetheinyl intermediate and in trans a free-standing oxy-FQF intermediate [either **1** or **2** (see Figure 5C)]. This functionality is in contrast to that traditionally observed for C domains embedded within a multimodular NRPS (e.g., Trp-specific module 2 of Af12080) that couple two T domain-tethered amino acyl intermediates (one upstream and one downstream of the C domain) via amide bond formation for chain elongation. For embedded C domains, the thioester carbonyl of the upstream intermediate acts as the electrophilic acceptor while the α-amino group of the downstream intermediate is activated to be nucleophilic. Path A of Figure 5C fits this paradigm for the upstream tethered intermediate as the electrophilic acceptor, but indole N1 of oxy-FQF (rather than an α-amino group) is the nucleophile for amide bond formation. The reaction between an upstream enzyme-bound thioester intermediate and free low-molecular weight nucleophile (*N*-hydroxyhistamine) has also been characterized in pseudomonine biosynthesis (*49*). Path B of Figure 5C reverses the roles of the two proposed reaction intermediates and also represents an N−C bond forming event unprecedented for C domain chemistry; the upstream tethered alanyl-S-Enz intermediate would be activated for nucleophilic attack on the electrophilic C2 atom of the bound oxy-FQF intermediate. In either case, the bicyclic indole moiety is thereby converted to the tricyclic imidazoindolone ring system.

Other Fungal Alkaloids That Are Biosynthesized in Part by Oxidative Acylation of Indole. The two-step process of Trp-derived indole oxidation and amino acid coupling described in this work for the conversion of FQF to FQA is likely shared among several families of fungal indolic natural products (Figure 2). The bioactivities of the compounds provided in Figure 2 include the mycotoxin tryptoquivaline, a tremor-causing metabolite originally isolated from *A. clavatus* (*50*, *51*); and potential therapeutics asperlicin, a cholecystokinin receptor antagonist from *Aspergillus alliaceus* (*52*, *53*), chaetominine, an antitumor agent more potent than 5-fluorouracil (*54*), fiscalin A, a substance P inhibitor from *N. fischeri* (*10*), and fumiquinazoline I, a weak antifungal agent from an *Acremonium* sp. (*9*). Compounds listed that do not have an attributed biological activity include the pyrazinoquinazolinone cottoquinazoline A from *A. versicolor* (*12*) and the diketopiperazine lumpidin from *Penicillium nordicum* (*55*). Of interest is the fact that in cases where bioactivities have been described for the natural product before and after amino acid coupling to the indolic scaffold (FQF vs FQA, fiscalin B vs fiscalin A, and asperlicin C vs asperlicin) the coupled product is reported to be 2−15-fold more potent (*5*, *10*, *53*).

Inspection of the compounds listed in Figure 2 provides possible insight into the mechanism of indole oxidation and dual N−C bond formation at N1′ and C2′ of the indole ring. Like that

observed for FQA (Figure 1B), the side of attack of the α-amino group of the coupled amino acid at C2′ is opposite the side observed for the hydroxyl group at C3′ for chaetominine, fumiquinazoline I, and asperlicin. In all these cases, the resulting stereochemistry across the C2′−C3′ bond could result from nucleophilic attack of an epoxyindole intermediate (e.g., path A, Figure 5C) or directional, "opposite-side" attack of a 3′-hydroxyiminium intermediate (e.g., path B, Figure 5C). In contrast, the stereochemistry across the C2′−C3′ bond for lumpidin, tryptoquivaline, fiscalin A, and cottoquinazoline A could be obtained only by attack of the α-amino group of the coupled amino acid at C2′ on the same side as the hydroxyl functionality at C3′ and not by an attack on an epoxyindole intermediate. This scenario suggests that a 3′-hydroxyiminium species is the likely intermediate prior to amino acid coupling to the indole scaffold of this group of fungal alkaloids.

Fumiquinazoline Biosynthetic Gene Cluster and Similar Clusters in Other Fungi. Our results characterizing the activities of Af12060 and Af12050 validate the identification of the fumiquinazoline biosynthetic gene cluster of *A. fumigatus* Af293. We anticipate that the fumiquinazoline cluster includes the trimodular NRPS Af12080, two putative FAD-dependent oxidoreductases (ORFs 12060 and 12070), a stand-alone monomodular NRPS (12050), an anthranilate synthase homologue (12110), a HET domain protein (12090), a nitrilase homologue (12100), and a putative MFS transporter (12040) (Figure 1A). Of note is the fact that the process for generating FQA from Ant, L-Trp, and L-Ala requires just three ORFs of this eight-gene cluster: Af12080, Af12050, and Af12060. This leaves an additional oxidoreductase (Af12070), a HET domain protein (Af12100), and a nitrilase/amidohydrolase homologue (Af12110) for other possible transformations. At least one additional enzyme, likely Af12070 or Af12100, is required to transform FQA into the naturally occurring fumiquinazolines C and D (Figure S1 of the Supporting Information), which appear to be formed via intramolecular cyclization between the imidazoindolone OH or NH group and C3 of the pyrazinoquinazolinone (*5*). The possible role of the putative HET domain protein [or homologue of HET-6^{OR} from *Neurospora crassa* (*56*)] is a much greater mystery. HET domain proteins are associated with mediating cell death in fungal vegetative (heterokaryon) incompatibility (*57*, *58*). A PSI-BLAST search with residues 1−250 of Af121090 as the query sequence indicates that there are seven HET domain genes in *A. fumigatus* Af293. It is tempting to speculate that the clustering of this ORF with the FQ biosynthetic machinery provides some link to FQ biological function, but it may be that the FQ biosynthetic gene cluster spans only ORFs 12040−12080.

As expected, an orthologous gene cluster is present in *A. fumigatus* CEA10 spanning AFUB_078010−AFUB_078100. The gene product for the amidohydrolase homologue has not been annotated but is present and 100% identical to AFUA_6g12100. Of greater potential interest is the presence of genes homologous to Af12080, Af12050, and Af12060 clustered in the genomes of *N. fischeri* NRRL181 and *A. clavatus* NRRL1. The *N. fischeri* homologues include NFIA_057960 (trimodular NRPS), NFIA_057990 (monomodular NRPS), and NFIA_057970 (FAD monooxygenase). *N. fischeri* is a known producer of mambers of the fiscalin family of quinazoline alkaloids (*10*); fiscalin A and FQA are highly similar, exhibiting two subtle differences: the stereochemistry at C2′ of the imidazoindolone and the C3 substituent of the pyrazinoquinazolinone core (methyl for FQA vs isopropyl for fiscalin A) (Figure S1 of the Supporting Information). The *N. fischeri* cluster contains a unique ORF between the monooxygenase and monomodular NRPS, a 2-oxoglutarate-Fe(II)-dependent oxidoreductase. In *A. clavatus* NRRL1, the homologous ORFs include ACLA_017890 (trimodular NRPS), ACLA_017900 (monomodular NRPS), and ACLA_017910 and ACLA_017920 (both FAD monooxygenases). In addition, this *A. clavatus* cluster contains an Af12070 homologue that resides immediately upstream of the trimodular NRPS. Characterized products from *A. clavatus* include the tryptoquivalines (*50*, *51*, *59*), which could arise from enzymatic processing of a fiscalin A-like precursor.

ORFs AFUA_6g12040−AFUA_6g12080 of the fumiquinazoline gene cluster are regulated by LaeA (*60*), a global regulator of several secondary metabolite pathways (*61*); loss of LaeA results in an *A. fumigatus* mutant with reduced virulence (*62*). Although there is no reported connection between the production of fumiquinazolines and *A. fumigatus* virulence, it is known that many secondary metabolites produced by filamentous fungi are important for their pathogenicity as toxins and immunosuppresants (*63*). However, there is no single factor (small molecule or gene product) that alone has been described as being essential and sufficient for *A. fumigatus* pathogenicity (*64*). Future studies aimed at understanding the biological function of FQs and their possible connection to the pathogenicity of *A. fumigatus* can now be undertaken.

In conclusion, the maturation of FQF to FQA in *A. fumigatus* Af293 is an oxidative, dual N−C bond-forming process previously unprecedented for NRPS-based logic. Oxidation of the pyrrole ring of FQF by the flavoprotein monooxygenase Af12060 is a prerequisite for alanine coupling to N1′ and C2′ of the oxidized indole by the monomodular tridomain NRPS Af12050. Overall, the four NRPS modules of the fumiquinazoline cluster (three modules of Af12080 and one module of Af12050) use two proteinogenic amino acids, L-Trp and L-Ala, and one nonproteinogenic amino acid, the aryl α-amino acid anthranilate, to build the hexacyclic FQA molecule in a short efficient pathway. This work validates the fumiquinazoline biosynthetic gene cluster of *A. fumigatus* Af293 and represents a biosynthetic oxidative-acylation transformation that may be shared among several families of bioactive fungal indolic alkaloids.

ACKNOWLEDGMENT

We thank the ICCB-Longwood Screening Facility at Harvard Medical School for access to their microwave reactor. We thank Thomas Gerken for providing *A. fumigatus* Af293 cDNA and Elizabeth Sattely for purified Sfp. We are grateful to Stuart Haynes for his careful reading of the manuscript.

SUPPORTING INFORMATION AVAILABLE

Discussion of the mass spectral characterization and [^{18}O]H_2O incorporation studies of the indoline-2′,3′-diol (**3**) and figures providing examples of fungal alkaloids containing a pyrazinoquinazolinone core scaffold (Figure S1), identification of FQF and FQA from *A. fumigatus* Af293 culture broth (Figure S2), SDS−PAGE gels of Ni-affinity-purified Af12060 and Af12050 (Figure S3), FAD binding by Af12060 (Figure S4), data characterizing synthetic FQF (Figure S5), ^{1}H NMR data for synthetic FQF (Figure S6), a spectrophotometric assay of NADPH consumption by Af12060 with or without Af12050 (Figure S7), characterization of **3** (Figure S8), characterization of the oxidized dimer of FQF (**4**) (Figure S9), data characterizing the enzymatic product FQA (Figure S10), ^{1}H NMR data for FQA (Figure S11),

data describing the enzymatic production of FQA analogue 1 (Figure S12), data describing the enzymatic reconstitution of FQA analogue 2 (Figure S13), and ^{1}H NMR data for glyantrypine (GAT) (Figure S14). This material is available free of charge via the Internet at http://pubs.acs.org.

REFERENCES

1. Bräse, S., Encinas, A., Keck, J., and Nising, C. F. (2009) Chemistry and biology of mycotoxins and related fungal metabolites. *Chem. Rev. 109*, 3903–3990.
2. D'Yakonov, A., and Telezhenetskaya, M. (1997) Quinazoline alkaloids in nature. *Chem. Nat. Compd. 33*, 221–267.
3. Mhaske, S. B., and Argade, N. P. (2006) The chemistry of recently isolated naturally occurring quinazolinone alkaloids. *Tetrahedron 62*, 9787–9826.
4. Avendano, C., and Menendez, J. C. (2003) Chemistry of pyrazino[2,1-b]quinazoline-3,6-diones. *Curr. Org. Chem. 7*, 149–173.
5. Takahashi, C.; et al. (1995) Fumiquinazolines A−G, novel metabolites of a fungus separated from a *Pseudolabrus* marine fish. *J. Chem. Soc., Perkin Trans. 1*, 2345–2353.
6. Frisvad, J. C., Rank, C., Nielsen, K. F., and Larsen, T. O. (2009) Metabolomics of *Aspergillus fumigatus*. *Med. Mycol. 47*, 53–71.
7. Larsen, T. O., Svendsen, A., and Smedsgaard, J. (2001) Biochemical characterization of ochratoxin A-producing strains of the genus *Penicillium*. *Appl. Environ. Microbiol. 67*, 3630–3635.
8. Han, X.-x., Xu, X.-y., Cui, C.-b., and Gu, Q.-q. (2007) Alkaloidal compounds produced by a marine-derived fungus, *Aspergillus fumigatus* H1-04, and their antitumor activities. *Zhongguo Yaowu Huaxue Zazhi 17*, 232–237.
9. Gilbert, N. B., Montserrat, A., Paul, R. J., William, F., and Matthias, K. (2000) Oxepinamides A-C and fumiquinazolines H-I: Bioactive metabolites from a marine isolate of a fungus of the genus *Acremonium*. *Chem.—Eur. J. 6*, 1355–1360.
10. Wong, S. M.; et al. (1993) Fiscalins: New substance P inhibitors produced by the fungus *Neosartorya fischeri*. Taxonomy, fermentation, structures, and biological properties. *J. Antibiot. 46*, 545–553.
11. Penn, J., Purcell, M., and Mantle, P. G. (1992) Biosynthesis of glyantrypine by *Aspergillus clavatus*. *FEMS Microbiol. Lett. 92*, 229–233.
12. Fremlin, L. J., Piggott, A. M., Lacey, E., and Capon, R. J. (2009) Cottoquinazoline A and cotteslosins A and B, metabolites from an Australian marine-derived strain of *Aspergillus versicolor*. *J. Nat. Prod. 72*, 666–670.
13. Larsen, T. O., Frydenvang, K., Frisvad, J. C., and Christophersen, C. (1998) UV-guided isolation of alantrypinone, a novel *Penicillium* alkaloid. *J. Nat. Prod. 61*, 1154–1157.
14. Barrow, C. J., and Sun, H. H. (1994) Spiroquinazoline, a novel substance P inhibitor with a new carbon skeleton, isolated from *Aspergillus flavipes*. *J. Nat. Prod. 57*, 471–476.
15. Larsen, T. O., Franzyk, H., and Jensen, S. R. (1999) UV-guided isolation of verrucines A and B, novel quinazolines from *Penicillium verrucosum* structurally related to anacine from *Penicillium aurantiogriseum*. *J. Nat. Prod. 62*, 1578–1580.
16. Leong, S.-l., Schnürer, J., and Broberg, A. (2008) Verrucine F, a quinazoline from *Penicillium verrucosum*. *J. Nat. Prod. 71*, 1455–1457.
17. Schwarzer, D., Finking, R., and Marahiel, M. A. (2003) Nonribosomal peptides: From genes to products. *Nat. Prod. Rep. 20*, 275–287.
18. Strieker, M., Tanovic, A., and Marahiel, M. A. (2010) Nonribosomal peptide synthetases: Structures and dynamics. *Curr. Opin. Struct. Biol. 20*, 234–240.
19. Eisfeld, K. (2009) Non-ribosomal peptide synthetases of fungi. In Physiology and Genetics, pp 305−330, Springer-Verlag, Berlin.
20. Keating, T. A.; et al. (2001) Chain termination steps in nonribosomal peptide synthetase assembly lines: Directed acyl-enzyme breakdown in antibiotic and siderophore biosynthesis. *ChemBioChem 2*, 99–107.
21. Du, L., and Lou, L. (2009) PKS and NRPS release mechanisms. *J. Nat. Prod. 27*, 255–278.
22. Walsh, C. T.; et al. (2001) Tailoring enzymes that modify nonribosomal peptides during and after chain elongation on NRPS assembly lines. *Curr. Opin. Chem. Biol. 5*, 525–534.
23. Samel, S. A., Marahiel, M. A., and Essen, L.-O. (2008) How to tailor non-ribosomal peptide products: New clues about the structures and mechanisms of modifying enzymes. *Mol. BioSyst. 4*, 387–393.
24. Latge, J.-P. (1999) *Aspergillus fumigatus* and aspergillosis. *Clin. Microbiol. Rev. 12*, 310–350.
25. Nierman, W. C.; et al. (2005) Genomic sequence of the pathogenic and allergenic filamentous fungus *Aspergillus fumigatus*. *Nature 438*, 1151–1156.
26. Fedorova, N. D.; et al. (2008) Genomic islands in the pathogenic filamentous fungus *Aspergillus fumigatus*. *PLoS Genet. 4*, e1000046.
27. Challis, G. L. (2008) Genome mining for novel natural product discovery. *J. Med. Chem. 51*, 2618–2628.
28. Ames, B. D., and Walsh, C. T. (2010) Anthranilate-activating modules from fungal nonribosomal peptide assembly lines. *Biochemistry 49*, 3351–3365.
29. Wilkins, M. R.; et al. (1999) Protein identification and analysis tools in the ExPASy server. *Methods Mol. Biol. 112*, 531–552.
30. Liu, J.-F.; et al. (2005) Three-component one-pot total syntheses of glyantrypine, fumiquinazoline F, and fiscalin B promoted by microwave irradiation. *J. Org. Chem. 70*, 6339–6345.
31. Quadri, L. E. N.; et al. (1998) Characterization of Sfp, a *Bacillus subtilis* phosphopantetheinyl transferase for peptidyl carrier protein domains in peptide synthetaseses. *Biochemistry 37*, 1585–1595.
32. Soding, J., Biegert, A., and Lupas, A. N. (2005) The HHpred interactive server for protein homology detection and structure prediction. *Nucleic Acids Res. 33*, W244–W248.
33. Greenhagen, B. T.; et al. (2008) Crystal structure of the pyocyanin biosynthetic protein PhzS. *Biochemistry 47*, 5281–5289.
34. van Berkel, W. J. H., Kamerbeek, N. M., and Fraaije, M. W. (2006) Flavoprotein monooxygenases, a diverse class of oxidative biocatalysts. *J. Biotechnol. 124*, 670–689.
35. Lawen, A., and Traber, R. (1993) Substrate specificities of cyclosporin synthetase and peptolide SDZ 214−103 synthetase. Comparison of the substrate specificities of the related multifunctional polypeptides. *J. Biol. Chem. 268*, 20452–20465.
36. Rausch, C., Weber, T., Kohlbacher, O., Wohlleben, W., and Huson, D. H. (2005) Specificity prediction of adenylation domains in nonribosomal peptide synthetases (NRPS) using transductive support vector machines (TSVMs). *Nucleic Acids Res. 33*, 5799–5808.
37. Finking, R., and Marahiel, M. A. (2004) Biosynthesis of nonribosomal peptides. *Annu. Rev. Microbiol. 58*, 453–488.
38. Ballou, D. P., Entsch, B., and Cole, L. J. (2005) Dynamics involved in catalysis by single-component and two-component flavin-dependent aromatic hydroxylases. *Biochem. Biophys. Res. Commun. 338*, 590–598.
39. Abe, I., and Prestwich, G. D. (1999) Squalene epoxidase and oxidosqualene:lanosterol cyclase: Key enzymes in cholesterol biosynthesis. In Comprehensive Natural Products Chemistry (Barton, D. H. R., and Nakanishi, K., Eds.) pp 267−298, Pergamon, Oxford, U.K.
40. Kovaleva, E. G., and Lipscomb, J. D. (2008) Versatility of biological non-heme Fe(II) centers in oxygen activation reactions. *Nat. Chem. Biol. 4*, 186–193.
41. Gillam, E. M. J., Notley, L. M., Cai, H., De Voss, J. J., and Guengerich, F. P. (2000) Oxidation of indole by cytochrome P450 enzymes. *Biochemistry 39*, 13817–13824.
42. Chauhan, N.; et al. (2009) Reassessment of the reaction mechanism in the heme dioxygenases. *J. Am. Chem. Soc. 131*, 4186–4187.
43. Heemstra, J. R., and Walsh, C. T. (2008) Tandem action of the O_2- and $FADH_2$-dependent halogenases KtzQ and KtzR produce 6,7-dichlorotryptophan for kutzneride assembly. *J. Am. Chem. Soc. 130*, 14024–14025.
44. Meyer, A., Wursten, M., Schmid, A., Kohler, H.-P. E., and Witholt, B. (2002) Hydroxylation of indole by laboratory-evolved 2-hydroxybiphenyl 3-monooxygenase. *J. Biol. Chem. 277*, 34161–34167.
45. Balibar, C. J., and Walsh, C. T. (2006) In vitro biosynthesis of violacein from L-tryptophan by the enzymes VioA-E from *Chromobacterium violaceum*. *Biochemistry 45*, 15444–15457.
46. Grubbs, A. W., Artman, G. D., III, Tsukamoto, S., and Williams, R. M. (2007) A concise total synthesis of the notoamides C and D. *Angew. Chem., Int. Ed. 46*, 2257–2261.
47. Ding, Y.; et al. (2010) Genome-based characterization of two prenylation steps in the assembly of the stephacidin and notoamide anticancer agents in a marine-derived *Aspergillus* sp. *J. Am. Chem. Soc. 132*, 12733–12740.
48. Yin, W.-B., Grundmann, A., Cheng, J., and Li, S.-M. (2009) Acetylaszonalenin biosynthesis in *Neosartorya fischeri*: Identification of the biosynthetic gene cluster by genomic mining and functional proof of the genes by biochemical investigation. *J. Biol. Chem. 284*, 100–109.
49. Sattely, E. S., and Walsh, C. T. (2008) A latent oxazoline electrophile for N-O-C bond formation in pseudomonine biosynthesis. *J. Am. Chem. Soc. 130*, 12282–12284.
50. Clardy, J., Springer, J. P., Buechi, G., Matsuo, K., and Wightman, R. (1975) Tryptoquivaline and tryptoquivalone, two tremorgenic metabolites of *Aspergillus clavatus*. *J. Am. Chem. Soc. 97*, 663–665.
51. Springer, J. P. (1979) The absolute configuration of nortryptoquivaline. *Tetrahedron Lett.*, 339–342.

52. Chang, R. S.; et al. (1985) A potent nonpeptide cholecystokinin antagonist selective for peripheral tissues isolated from *Aspergillus alliaceus*. *Science 230*, 177–179.
53. Goetz, M. A.; et al. (1988) Novel cholecystokinin antagonists from *Aspergillus alliaceus*. I. Fermentation, isolation, and biological properties. *J. Antibiot. 41*, 875–877.
54. Jiao, R. H.; et al. (2006) Chaetominine, a cytotoxic alkaloid produced by endophytic *Chaetomium* sp. IFB-E015. *Org. Lett. 8*, 5709–5712.
55. Larsen, T. O., Petersen, B. O., and Duus, J. O. (2001) Lumpidin, a novel biomarker of some ochratoxin A producing Penicillia. *J. Agric. Food Chem. 49*, 5081–5084.
56. Smith, M. L.; et al. (2000) Vegetative incompatibility in the het-6 region of *Neurospora crassa* is mediated by two linked genes. *Genetics 155*, 1095–1104.
57. Glass, N. L., and Dementhon, K. (2006) Non-self recognition and programmed cell death in filamentous fungi. *Curr. Opin. Microbiol. 9*, 553–558.
58. Paoletti, M., and Clave, C. (2007) The fungus-specific HET domain mediates programmed cell death in *Podospora anserina*. *Eukaryotic Cell 6*, 2001–2008.
59. Buechi, G., Luk, K. C., Kobbe, B., and Townsend, J. M. (1977) Four new mycotoxins of *Aspergillus clavatus* related to tryptoquivaline. *J. Org. Chem. 42*, 244–246.
60. Perrin, R. M.; et al. (2007) Transcriptional regulation of chemical diversity in *Aspergillus fumigatus* by LaeA. *PLoS Pathog. 3*, e50.
61. Bok, J. W., and Keller, N. P. (2004) LaeA, a regulator of secondary metabolism in *Aspergillus* spp. *Eukaryotic Cell 3*, 527–535.
62. Bok, J. W.; et al. (2005) LaeA, a regulator of morphogenetic fungal virulence factors. *Eukaryotic Cell 4*, 1574–1582.
63. Sexton, A. C., and Howlett, B. J. (2006) Parallels in fungal pathogenesis on plant and animal hosts. *Eukaryotic Cell 5*, 1941–1949.
64. Rementeria, A.; et al. (2005) Genes and molecules involved in *Aspergillus fumigatus* virulence. *Rev. Iberoam. Micol. 22*, 1–23.